Optical Dot Gain in a Halftone Print

Geoffrey L. Rogers
Matrix Clock, 26 E33 St, New York, New York 10016

Abstract

The scattering of light within paper can affect the tone characteristics of a printed halftone image. A halftone image is formed by variation in the average reflectance, which is determined by the size of the ink dots. Photon migration within the paper from noninked to inked regions tends to increase the photon absorption and thus decrease the halftone reflectance—the dots are effectively larger than their physical size. This effect is known as optical dot gain or as the Yule-Nielson effect. The degree of optical dot gain depends on the distance that the photons migrate within the paper, which in turn depends on the paper's scattering and absorption characteristics, and on the thickness of the paper. We develop a theory that expresses the halftone reflectance in terms of the halftone microstructure—the screen period, dot size, dot shape, and ink transmission—and the effects due to the paper. The paper effects are represented in the theory by a point spread function, which is a conditional probability density that characterizes the photon migration within the paper, and by the paper's reflectance. We construct a model of photon transport within the paper by solving the transport equation using a diffusion approximation, from which we derive a point spread function. We interpret the expanded Murray–Davies model of halftone reflectance in terms of the theory developed here by giving a probabilistic interpretation to optical dot gain. We show that optical dot gain can be related to a single numerical parameter. Using the diffusion point spread function, we show how this parameter is related to the physical quantities that characterize the paper.

Introduction

Recently there has been interest in the scattering of light within paper and the effect this scattering has on the tone characteristics of a printed halftone image.[1–6] A halftone image is formed by variation in the halftone reflectance, which is determined by the size of the ink dots. Photon migration within the paper, from noninked to inked regions, tends to increase the photon absorption and thus decrease the halftone reflectance—the dots are effectively larger than their physical size. This effect is known as optical dot gain, or as the Yule-Nielson effect, and depends on the characteristics of the paper. This effect is particularly pronounced when the distance the photons migrate is comparable to the screen period.

In the first part of this article, we develop a theory that expresses the halftone reflectance in terms of the halftone micro-structure—the screen period, dot size, dot shape, and ink transmission—and the effects due to the paper. The paper effects are represented in the theory by a point spread function (PSF), which is a conditional probability density that characterizes the photon migration within the paper. It is shown that the effect that light scatter has on the halftone reflectance can be expressed in terms of a single quantity—a factor we call Z. This factor is a function of the dot shape, dot size, screen period, and the paper's PSF.

The paper's point spread function characterizes the photon migration within the paper, which depends on the paper's scattering and absorption characteristics, and on the thickness of the paper. In the second part of the article, we construct a model of photon transport within the paper by solving the transport equation using a diffusion approximation.[7,8] From this we derive the diffusion point spread function.

Using the diffusion PSF, we show plots of the halftone reflectance for several typical values of the paper's parameters. We introduce a phenomenological expression for Z with one adjustable parameter and comparisons are made between the phenomenological Z and the exact Z as calculated with the diffusion PSF.

In the third part of the article, we interpret the expanded Murray–Davis model[4] of halftone reflectance in terms of the theory developed here by giving a probabilistic interpretation of optical dot gain—the various processes that give rise to optical dot gain are described in terms of probabilities. We show that Z can be interpreted as a probability: the conditional probability that a photon emerges from the paper through a dot if it originally entered the paper through a dot. We show that all other probabilities describing the effects of optical dot gain can be obtained from this "dot–dot" probability.

Halftone Reflectance

In the following, we obtain an expression for the halftone reflectance (the average reflectance) from a region of the halftone print, in terms of the halftone microstructure—the ink transmission and the size and shape of the ink dots—and the effects of the paper.

The ink is laid onto the paper in the form of circular dots with radius d, and the dot centers fall on a square grid array (screen grid) with screen period r. We consider a region of the halftone image that has a constant tone, i.e., the size of the dots is constant over the region and the region is large compared to the screen period.

The average reflectance is found by averaging the point reflectance over the region:

$$\overline{R} = \frac{1}{(Nr)^2} \int_{(\text{region})} R(x,y)\,dA, \qquad (1)$$

where $dA = dx\,dy$ is an element of area, N^2 is the number of dots in the region, and $(Nr)^2$ is the area of the region. The region consists of N^2 cells of area r^2, and each cell contains one dot. (For simplicity, in all that follows, we take the limit $N \to \infty$.)

The point reflectance $R(x,y)$ is the reflectance at the point (x,y) and is given by[9]:

$$R(x,y) = R_p T(x,y)\int_{-\infty}^{\infty}\int_{-\infty}^{\infty} T(x',y')H(x-x',y-y')dx'dy'. \quad (2)$$

The quantity $H(x-x', y-y'$ is the point spread function, and $R_pH(x-x', y-y')$ is the probability per unit area that a photon entering the surface of the paper at point (x',y') exits the paper at a point (x,y). The bare paper has diffuse reflectance of R_p, so $H(x,y)$ is normalized to unity. It is assumed that the paper is isotropic, so $H(x,y)$ is radially symmetric:

$$H(x,y) = H\left(\sqrt{x^2+y^2}\right) = H(\rho),$$

where ρ is the polar radial coordinate.

The transmission function $T(x,y)$ is the transmittance of the ink layer at point (x,y). Certainly, those areas of the paper between the dots (no ink) have transmission of 1. The areas covered by ink have a transmission T_0. One can express the transmission function as:

$$T(x,y) = 1 - (1 - T_0)\,C(x,y), \quad (3)$$

where the function $C(x,y)$ is 1 if there is ink at x,y and 0 if there is no ink at x,y. This function is a convolution of the distribution function for the dots, and a function that describes the shape of the dots:

$$C(x,y) = \mathrm{circ}\left[\frac{\sqrt{x^2+y^2}}{d}\right] * g, \quad (4)$$

where the * indicates a convolution. The distribution function for the dots $g(x,y)$ is:

$$g(x,y) = \sum_{n,m}\delta(x-nr)\delta(y-mr), \quad (5)$$

where r is the dot spacing (screen period) and $d(x)$ is a Dirac delta function. The circ $[u/d]$ is the shape function for circular dots and is defined by:

$$\mathrm{circ}[u/d] = \begin{cases}1, & u \le d\\ 0, & u > d\end{cases}, \quad (6)$$

with d the radius of the dots. Thus, the expression

$$C(x,y) = \sum_{n,m}\mathrm{circ}\left[\frac{\sqrt{(x-nr)^2+(y-mr)^2}}{d}\right]$$

is equal to 0 for those points (x,y) where there is no ink, and is equal to 1 for those points where there is ink.

Expanding Eq. 2 using Eq. 3 one obtains for the point reflectance:

$$\begin{aligned}R(x,y) &= [1-(1-T_0)\,C(x,y) - (1-T_0)P(x,y)\\ &\quad + (1-T_0)^2\,C(x,y)\,P(x,y)]\,R_p,\end{aligned} \quad (7)$$

where $P(x,y)$ is defined as:

$$P(x,y) = \int\int C(x'y')H(x-x',y-y')dx'\,dy'. \quad (8)$$

The quantity $P(x,y)$ is a double convolution and can be evaluated by taking the inverse Fourier transform of the product of the Fourier transforms of the convolution operands.

The Fourier transform of $P(x,y)$ is

$$F\{P(x,y)\} = F\{\mathrm{circ}[\rho/d]\}F\{g(x,y)\}F\{H(x,y)\}. \quad (9)$$

The Fourier transform of circ [ρ/d] is readily obtained[10]:

$$F\{\mathrm{circ}[\rho/d]\} = d^2\,\frac{J_1(2\pi kd)}{kd}, \quad (10)$$

where $J_1(x)$ is a first-order Bessel function k is the magnitude of the two-dimensional spatial frequency (in cycle/unit length).

The Fourier transform of the dot distribution $g(x,y)$ is also readily obtained:

$$F\{g(x,y)\} = \frac{1}{r^2}\sum_{n,m}\delta(k_x - n/r)\delta(k_y - m/r), \quad (11)$$

where k_x and k_y are the x and y components of the spatial frequency.

The Fourier transform of $H(x,y)$ is the optical transfer function (OTF) of the paper.[11] Because of the assumed symmetry and reality of $H(x,y)$, the paper's OTF is identical to its modulation transfer function (MTF) and is radially symmetric in frequency space:

$$\tilde{H}(k) = F\{H(x,y)\}, \quad (12)$$

where we define $\tilde{H}(k)$ as the MTF of the paper.

Taking the inverse Fourier transform of Eq. 9, one obtains for $P(x,y)$:

$$P(x,y) = \frac{\pi d^2}{r^2}\sum_{n,m} I_{nm}\tilde{H}_{nm}\exp[-2\pi i(nx+my)/r], \quad (13)$$

where we define

$$J_{nm} = \frac{J_1\left(2\pi\sqrt{n^2+m^2}\,d/r\right)}{\pi\sqrt{n^2+m^2}\,d/r} \quad (14)$$

and

$$\tilde{H}_{nm} = \tilde{H}(\sqrt{n^2+m^2}\,/\,r). \tag{15}$$

Note that $J_{00} = \tilde{H}_{00} = 1$.

One obtains the halftone, or average, reflectance from the region by averaging the point reflectance $R(x,y)$ over all x,y. Using Eq. 7 in Eq. 1, there are four terms to integrate. The first term is clearly equal to 1. The second term is:

$$\begin{aligned}&(1-T_0)\frac{1}{(Nr)^2}\int\int \mathrm{circ}\left[\frac{\sqrt{x^2+y^2}}{d}\right] * g\ dx\,dy = \\ &(1-T_0)\pi(d/r)^2.\end{aligned} \tag{16}$$

The third term is:

$$\begin{aligned}&(1-T_0)\frac{1}{(Nr)^2}\int\int P(x,y)\ dx\,dy = \\ &(1-T_0)\pi(d/r)^2,\end{aligned} \tag{17}$$

because $H(x,y)$ is normalized to 1.

The fourth term is:

$$\begin{aligned}&(1-T_0)^2\frac{1}{(Nr)^2}\int\int \mathrm{circ}\left[\frac{\sqrt{x^2+y^2}}{d}\right] * g\ P(x,y)\ dx\,dy = \\ &= \frac{\pi(d/r)^2}{(Nr)^2}(1-T_0)^2\sum_{n,m,n'm'} J_{nm}\tilde{H}_{nm} \\ &\times\int\int \mathrm{circ}\left[\frac{(x-n'r)^2+(y-m'r)^2}{d}\right]\exp[-2\pi i(nx+my)/r]dx\ dy.\end{aligned}$$

Substituting $u = x - n'r$ and $v = y - m'r$ the double integral above can be written:

$$\begin{aligned}&\exp[-2\pi i(nn'+mm')]\int\int \mathrm{circ}\left[\frac{\sqrt{u^2+v^2}}{d}\right] \\ &\times\exp[2\pi i(nu+mv)/r]du\ dv.\end{aligned} \tag{19}$$

The first exponential is equal to 1 for all n,m,n',m', and the double integral is identically $\pi d^2 J^*_{nm}$, so that the fourth term is

$$\pi^2(d/r)^4(1-T_0)^2\sum_{n,m}|J_{nm}|^2\tilde{H}_{nm}. \tag{20}$$

Thus, one writes the average reflectance from the region as

$$\overline{R} = R_p\left[1-2\mu(1-T_0)+\mu^2(1-T_0)^2 Z\right], \tag{21}$$

where μ is the fractional area covered by the dots* $\mu = \pi(d/r)^2$, and

$$Z = \sum_{n,m}|I_{nm}|^2\tilde{H}_{nm}, \tag{22}$$

The series Z completely contains the effects of the optical dot gain. It is a function of dot shape, dot size, screen period, and the scattering characteristics of the paper. It is shown in the section on Dot and Nondot Reflectance that μZ is the probability that a photon exits the paper through a dot if it originally entered through a dot and that one can interpret Z^{-1} as an effective scattering area.

Although the expression for $\overline{R}$ has been derived for circular dots, the average reflectance has the same form as Eq. 21 for dots of any shape, with Z given by Eq. 22 and the definition of J_{nm} generalized. If the dots have a shape function given by $w(x,y)$, and lie on a grid with period r, then one defines J_{nm} as

$$J_{nm} = \frac{\int\int w(x,y)\exp[2\pi i(nx+my)/r]dx\ dy}{\int\int w(x,y)dx\ dy}. \tag{23}$$

For example, if the dots are square with sides of length d, then $w(x,y) = \mathrm{rect}(x/d)\,\mathrm{rect}(y/d)$, where $\mathrm{rect}(u) = 1$ if $|u| \le 1/2$ and zero otherwise, and

$$J_{nm} = \mathrm{sinc}\,(nd/r)\ \mathrm{sinc}\,(md/r),$$

with $\mathrm{sinc}\,(v) = \sin(\pi v)/(\pi v)$.

To give the expression for $\overline{R}$ a physical meaning, we consider two extreme cases: the lateral scattering length is much larger than the screen period and the lateral scattering length is much smaller than the screen period. (We set $R_p = 1$ for simplicity.) The lateral scattering length is defined as the first moment of $H(\rho)$,

$$\langle\rho\rangle = \int \rho H(\rho)dA, \tag{24}$$

and is the average lateral distance a photon travels. The value $1/\langle\rho\rangle$ is approximately the spatial bandwidth of the paper.

If $\langle\rho\rangle$ is much larger than the grid length, $\langle\rho\rangle/r > 1$, then $\tilde{H}(k) \approx 0$ for $k \ge 1/r$. Therefore, $\tilde{H}_{nm} \approx 0$ for $n,m \ne 0$, and

$$Z \approx 1. \tag{25}$$

The average reflectance in this case is

$$\begin{aligned}\overline{R} &= 1-2(1-T_0)\mu+(1-T_0)^2\mu^2 = \\ &= [1-\mu(1-T_0)]^2.\end{aligned} \tag{26}$$

The reflectance of the ink is $R_i = T_0^2$ (the paper reflectance is taken to be 1), so the average reflectance can be expressed as:

$$\overline{R} = [1-\mu(1-R_i^{1/2})]^2, \tag{27}$$

which is the Yule-Nielson equation[6] with $n = 2$. One can interpret this equation in terms of probabilities by writing it as

* This expression for Z with J_{nm} given by Eq. 14 is strictly correct only for $d \le r/2$ (or $\mu < \pi/4$), such that no dot overlap occurs. For $\pi/4 < \mu \le 1$, then $\mu = (\pi/2 - 2\theta + \sin 2\theta)/(1 + \cos 2\theta)$ with $\cos\theta = 2/(2d)$, and J_{nm} is somewhat different from Eq. 14, but can be readily calculated from Eq. 23.

$$\overline{R} = \mu R_i^{1/2}\left[(1-\mu)+\mu R_i^{1/2}\right]+ \\ (1-\mu)\left[(1-\mu)+\mu R_i^{1/2}\right]. \tag{28}$$

One can interpret $\overline{R}$ as the probability that an incident photon is reflected from the paper, $\mu R_i^{1/2}$ as the probability that the photon enters the paper through an inked area, and $(1 - \mu)$ as the probability the the photon enters the paper through a noninked area. The photon is said to be "completely" scattered if the probability that it exits through an inked or noninked area is proportional to the ink and noninked areas and is independent of whether the photon entered through an inked or noninked area, as indicated in Eq. 28. The first term on the right represents light entering the paper through an inked area and the second term represents light entering the paper through noninked regions. For both, after entering the paper, the light is "completely" scattered, and exits through a nondot region with probability $1 - \mu$ and through a dot with probability $\mu R^{1/2}$. That $Z \approx 1$ indicates that the light is completely scattered and a high degree of optical dot gain exists. This interpretation is generalized in the section on Dot and Nondot Reflectance.

If the lateral scattering length is very small compared to the grid length, $\langle\rho\rangle / r \to 0$, then $\tilde{H}(k) \approx 1$ for all $k < 1/\langle\rho\rangle \to \infty$. Then $\tilde{H}_{nm} \approx 1$ for all relevant n,m, and $Z \approx \sum_{n,m}|J_{nm}|^2$. This sum can be evaluated exactly by using the definition of J_{nm}, Eq. 23, and noting that $|w(x,y)|^2 = w(x,y)$, $\sum \exp[2\pi in(x - x')/r] = r\delta(x - x')$, and $\int w(x,y)\, dx\, dy = \pi d^2$. One finds

$$Z \approx 1/\mu. \tag{29}$$

The average reflectance in this case is

$$\overline{R} = 1-\mu(1-R_i). \tag{30}$$

This is the Murray–Davies equation,[4,12] the average reflectance without scattering within the paper, which is the Yule-Nielson equation with $n = 1$. In this case no optical dot gain occurs.

Photon Transport and the Diffusion PSF

In this section we obtain the distribution function for the photons within the paper by solving the transport equation using a diffusion approximation.[13,14,15,16,17,18,19,20] The photon distribution is then used to construct a diffusion point spread function.

The diffusion approximation assumes that any photon current is due only to gradients in the photon density. A number of authors[13,14,20] have discussed the conditions under which this approximation is valid: (1) that the albedo be close to 1 and (2) that the average distance that light travels in the medium be greater than the transport mean free path or, equivalently, that the optical thickness be greater than 1. As discussed below, these conditions are amply satisfied by most papers. Groenhuis et al.[13] compared the diffusion approximation to a Monte Carlo calculation, and found excellent agreement for the range of parameters we use here.

Paper consists of a very complex network of layered cellulose fibers plus filler pigments such as titanium dioxide or calcium carbonate.[21] The transparent, flattened fibers have ~75 µm width, ~8 µm thickness,[22] and an index of refraction[23] $n \approx 1.5$ so that light is scattered as it enters and exits a fiber as well as being internally reflected within the fiber. The thickness of paper (newsprint or bond) is typically 10 to 18 fiber layers.[22] The degree of absorption within white paper is quite small—the paper opacity is due to scattering.

Our model treats the paper in a simplified way. We ignore fiber orientation,[22] and multilayer structure,[24] and we assume that the paper is isotropic and homogeneous. The validity of these assumptions is discussed in the conclusion. We do not consider the fiber network as such, but we characterize the paper by its thickness and by two experimentally determined parameters that characterize scattering and absorption. In the section on Halftone Reflectance with Diffusion PSF, we indicate how these parameters can be measured. Our analysis assumes uncoated paper, but the model can be adjusted in a simple way to include coated paper.[21] As most papers consist of approximately equal volumes of cellulose and air,[21] we consider the "paper medium" to be cellulose with index $n = 1.5$ and that the photons scatter at the fiber–air boundaries within the paper.

In our model, photons are incident on the paper surface at a single point and these injected photons are scattered within the paper. We calculate the distribution of these scattered, nearly diffuse, photons. The diffusion point spread function is the normalized outward flux of these diffuse photons as a function of the distance from the point of incidence.

Because of the symmetry, we work in cylindrical coordinates ρ, z, ϕ and choose the $+z$ axis perpendicular to and pointing into the paper surface (pointing downward), with $z = 0$ on the paper top surface, the side from which the light is incident. The light is incident on the point $z = 0$, $\rho = 0$, and is traveling in the $+z$ direction. The paper has thickness t, so the bottom surface of the paper is at $z = +t$.

Our model treats photons as billiard balls undergoing elastic collisions with stationary scatterers and traveling at the speed c between collisions. We assume any interference effects average to zero. All the material quantities are wavelength independent, consistent with our assumption of "white" paper and "black" ink. The quantities that describe the photon flux are implicitly wavelength dependent, and for simplicity we assume arbitrary monochromatic radiation.

Diffusion Equation

We assume that a stream of photons traveling in the $+z$ direction is incident on the paper at the origin. The scattering of these injected photons is the source of the diffuse photons.

We start with the steady-state transport equation for the photon distribution[7]

$$\hat{\mathbf{s}} \cdot \nabla f(\mathbf{r},\hat{\mathbf{s}}) = \\ -\gamma_t f(\mathbf{r},\hat{\mathbf{s}}) + \frac{\gamma_s}{4\pi}\int_{(4\pi)} p(\hat{\mathbf{s}},\hat{\mathbf{s}}')f(\mathbf{r},\hat{\mathbf{s}}')d\Omega', \tag{31}$$

where $f(\mathbf{r},\hat{\mathbf{s}})$, the photon distribution, is the number of photons per unit volume per unit solid angle at position $\mathbf{r}$ travelling in direction $\hat{\mathbf{s}}$. This is related to the specific intensity $I(\mathbf{r},\hat{\mathbf{s}})$ (power per unit area per unit solid angle) as $I(\mathbf{r},\hat{\mathbf{s}}) = c\varepsilon f(\mathbf{r},\hat{\mathbf{s}})$ where e is the energy of the monochromatic photons. Below we separate the photon distribution function into two parts: one part describing the injected photons and the other the diffuse photons. The extinction coefficient is: $\gamma_t = \gamma_s + \gamma_a$ with γ_s, γ_a the scattering and the absorption coefficients, respectively. The phase function $p(\hat{\mathbf{s}},\hat{\mathbf{s}}')$ is the normalized differential scattering cross section and is the probability per unit solid angle that a photon originally traveling in direction $\hat{\mathbf{s}}'$ is traveling in direction $\hat{\mathbf{s}}$ after scattering. The phase function is normalized such that $1/(4\pi)\int p(\hat{\mathbf{s}},\hat{\mathbf{s}}')d\Omega' = 1$ and depends only on the angle between $\hat{\mathbf{s}}$ and $\hat{\mathbf{s}}'$: $p(\hat{\mathbf{s}},\hat{\mathbf{s}}') = p(\hat{\mathbf{s}}\bullet\hat{\mathbf{s}}')$. Following Groenhuis et al.,[13] we choose a phenomenological phase function that consists of a term representing isotropic scattering and a term that represents forward scattering

$$p(\hat{\mathbf{s}},\hat{\mathbf{s}}') = (1-g) + 4\pi g\delta(\hat{\mathbf{s}}\cdot\hat{\mathbf{s}}'-1), \tag{32}$$

where g is the average cosine of the scattering angle, $g \equiv \langle\hat{\mathbf{s}}\cdot\hat{\mathbf{s}}'\rangle = \int p(\hat{\mathbf{s}}\cdot\hat{\mathbf{s}}')\hat{\mathbf{s}}\cdot\hat{\mathbf{s}}'\,d\Omega$. The value g is an anisotropy parameter: $g = 1$ indicates the scattering is forwardly peaked, $g = 0$ indicates isotropic scattering, and $g = -1$ indicates the scattering is backwardly peaked. Separating the forward scattered part from the isotropic part enables one to separate the photon distribution into a diffuse distribution that consists of photons whose initial injected velocity has relaxed and a distribution of photons that have their initial injected velocities.

Using the phenomenological expression for $p(\hat{\mathbf{s}}\bullet\hat{\mathbf{s}}')$, the transport equation can be written

$$\hat{\mathbf{s}}\cdot\nabla f(\mathbf{r},\hat{\mathbf{s}}) = -\gamma_{tr}\, f(\mathbf{r},\hat{\mathbf{s}}) + \frac{\gamma_s'}{4\pi}\int_{(4\pi)} f(\mathbf{r},\hat{\mathbf{s}}')d\,\Omega', \tag{33}$$

where the transport coefficient, γ_{tr}, is defined by

$$\gamma_{tr} = \gamma_s' + \gamma_a \tag{34}$$

with the effective scattering coefficient $\gamma_s' = \gamma_s(1-g)$. The transport coefficient is the inverse of the transport mean free path $l^* = 1/\gamma_{tr}$,[18] which is the distance over which a photon's velocity relaxes, and is proportional to the paper's optical thickness $\tau = \gamma_{tr}t$.

The photon distribution is separated into two parts: a term representing the unscattered and forward scattered injected photons $f_i(\mathbf{r},\hat{\mathbf{s}})$ and a term representing the (nearly) diffuse photons $f_d(\mathrm{r}, \hat{\mathbf{s}})$

$$f(\mathbf{r},\hat{\mathbf{s}}) = f_i(\mathbf{r},\hat{\mathbf{s}}) + f_d(\mathbf{r},\hat{\mathbf{s}}), \tag{35}$$

where $f_d(\mathrm{r}, \hat{\mathbf{s}})$ describes those photons scattered such that their initial injected velocity has relaxed and $f_i(\mathrm{r}, \hat{\mathbf{s}})$ describes those photons that have essentially the same velocities with which they were injected.

Inserting Eq. 35 into Eq. 33 one sees that the injected photon distribution satisfies

$$\frac{d}{dz}f_i(\mathbf{r},\hat{\mathbf{s}}) = -\gamma_{tr}f_i(\mathbf{r},\hat{\mathbf{s}}),$$

so that the distribution of injected photons is

$$f_i(\mathbf{r},\hat{\mathbf{s}}) = \frac{S_0\delta(\rho)}{c2\pi\rho}\exp(-\gamma_{tr}z)\frac{\delta(\hat{\mathbf{s}}\cdot\hat{\mathbf{k}}-1)}{2\pi}, \tag{36}$$

where $\hat{\mathbf{k}}$ is a unit vector along the $+z$ axis and S_0 is the number of photons per unit time injected.

The transport equation for the diffuse photon distribution is

$$\hat{\mathbf{s}}\cdot\nabla f_d(\mathbf{r},\hat{\mathbf{s}}) = -\gamma_{tr}f_d(\mathbf{r},\hat{\mathbf{s}}) + \frac{\gamma_s'}{4\pi}\int_{(4\pi)}f_d(\mathbf{r},\hat{\mathbf{s}}')d\Omega' + \frac{1}{4\pi c}S(\mathbf{r}), \tag{37}$$

where the source term for the diffuse photons is

$$\begin{aligned} S(\mathbf{r}) &= c\gamma_s'\int_{(4\pi)}f_i(\mathbf{r},\hat{\mathbf{s}}')\,d\Omega' = \\ &\gamma_s' S_0\frac{\delta(\rho)}{2\pi\rho}\exp(-\gamma_{tr}z). \end{aligned} \tag{38}$$

One makes the diffusion approximation by expanding the diffuse photon distribution in a series of spherical harmonics and keeping only the first four terms: the $l = 0$, $m = 0$; and the $l = 1$, $m = -1, 0, 1$ terms. One can then write $f_d(\mathbf{r}, \hat{\mathbf{s}})$ as

$$f_d(\mathbf{r},\hat{\mathbf{s}}) = \frac{1}{4\pi}u(\mathbf{r}) + \frac{3}{4\pi c}\mathbf{j}(\mathbf{r})\cdot\hat{\mathbf{s}}, \tag{39}$$

where $u(\mathbf{r})$ is the diffuse photon density (number of photons per unit volume) and is equal to

$$u(\mathbf{r}) = \int_{(4\pi)}f_d(\mathbf{r},\hat{\mathbf{s}})\,d\Omega, \tag{40}$$

and $\mathbf{j}(\mathbf{r})$ is the diffuse photon current density (number of photons per unit area per unit time) and is equal to

$$\mathbf{j}(\mathbf{r}) = c\int_{(4\pi)}f_d(\mathbf{r},\hat{\mathbf{s}})\hat{\mathbf{s}}\,d\Omega. \tag{41}$$

Integrating Eq. 37 over all solid angles, one obtains a continuity equation

$$\nabla\cdot\mathbf{j}(\mathbf{r}) + \gamma_a c u(\mathbf{r}) = S(\mathbf{r}). \tag{42}$$

Multiplying Eq. 37 by $\hat{\mathbf{s}}$, using Eq. 39 for $f_d(\mathrm{r}, \hat{\mathbf{s}})$ and integrating over all solid angles, one obtains

$$\mathbf{j}(\mathbf{r}) = -\frac{c}{3\gamma_{tr}}\nabla u(\mathbf{r}). \tag{43}$$

This expression characterizes the diffusion approximation—the photon current is due only to the gradient in the photon density.

Combining Eqs. 42 and 43 and defining the diffusion coefficient $D = cl^*/3 = c/(3\gamma_{tr})$, one obtains the diffusion equation

$$D\nabla^2 u(\mathbf{r}) - c\gamma_a u(\mathbf{r}) = -S(\mathbf{r}). \tag{44}$$

In the following, we solve this equation, with appropriate boundary conditions, by constructing a Green's function.

Boundary Conditions

There are two boundaries, the top surface and the bottom surface of the paper. (Note that we choose the +z axis pointing downward.) Photons are incident on the paper top surface at one point, the origin. Away from the origin, there is no inward photon flux on the top or the bottom surface, only an outward flux of the internally scattered photons. There is, however, some internal reflection at the boundaries. This internal reflection can be considered an inward traveling flux equal to the outgoing flux times the Fresnel reflectance.[19]

We define the partial photon currents $\mathbf{j}_+(\rho, z)$ and $\mathbf{j}_-(\rho, z)$

$$\mathbf{j}_+(\rho,z) = c\int_{0\le\theta\le\pi/2} f(\rho,z;\hat{\mathbf{s}})\hat{\mathbf{s}}d\Omega \tag{45}$$

and

$$\mathbf{j}_-(\rho,z) = c\int_{\pi/2\le\theta\le\pi} f(\rho,z;\hat{\mathbf{s}})\hat{\mathbf{s}}d\Omega, \tag{46}$$

where $\mathbf{j}(\rho, z) = \mathbf{j}_+(\rho, z) + \mathbf{j}_-(\rho, z)$. Using Eq. 39 in Eqs. 45 and 46, one can express $\mathbf{j}_\pm$ as

$$\mathbf{j}_\pm(\rho,z) = \pm\frac{c}{4}\hat{\mathbf{k}}u(\rho,z) + \frac{1}{2}\mathbf{j}(\rho,z) \tag{47}$$

or, using Eq. 43

$$\mathbf{j}_\pm(\rho,z) = \pm\frac{c}{4}\hat{\mathbf{k}}\,u(\rho,z) - \frac{D}{2}\nabla u(\rho,z), \tag{48}$$

where $\hat{\mathbf{k}}$ is a unit vector pointing in the +z direction.

As indicated above, there is no external inward flux except at the origin. However, the internally reflected flux can be treated as incoming flux at the boundary, i.e., the flux directed inward at the paper surface is equal to the reflected part of the outwardly directed flux. In the Appendix, we show that this internal reflection can be approximated by an effective Fresnel reflection coefficient R_F, so that the boundary conditions are

$$\hat{\mathbf{k}}\cdot\mathbf{j}_+(\rho,0) = R_F\hat{\mathbf{k}}\cdot\mathbf{j}_-(\rho,0) \tag{49}$$

for the top surface and for the bottom surface

$$\hat{\mathbf{k}}\cdot\mathbf{j}_-(\rho,t) = R_F\hat{\mathbf{k}}\cdot\mathbf{j}_+(\rho,t), \tag{50}$$

where we assume a black (or no) backing. Using Eqs. 47 and 43, one can express the boundary conditions as

$$\begin{aligned}&\frac{c}{4}u(\rho,0) - \frac{D}{2}\frac{\partial}{\partial z}u(\rho,z)\Big|_{z=0} = \\ &= R_F\left[\frac{c}{4}u(\rho,0) + \frac{D}{2}\frac{\partial}{\partial z}u(\rho,z)\Big|_{z=0}\right]\end{aligned} \tag{51}$$

for the top surface and

$$\begin{aligned}&\frac{c}{4}u(\rho,t) + \frac{D}{2}\frac{\partial}{\partial z}u(\rho,z)\Big|_{z=t} = \\ &= R_F\left[\frac{c}{4}u(\rho,t) - \frac{D}{2}\frac{\partial}{\partial z}u(\rho,z)\Big|_{z=t}\right]\end{aligned} \tag{52}$$

for the bottom surface. Thus, one obtains a mixed homogeneous boundary condition for the top surface

$$u(\rho,0) - \frac{t}{\tau\delta}\frac{\partial}{\partial z}u(\rho,z)\Big|_{z=0} = 0 \tag{53}$$

and for the bottom surface

$$u(\rho,t) + \frac{t}{\tau\delta}\frac{\partial}{\partial z}u(\rho,z)\Big|_{z=t} = 0, \tag{54}$$

where τ is the optical thickness

$$\tau = \gamma_{tr}t \tag{55}$$

and d is defined as

$$\delta = \frac{3}{2}\frac{1-R_F}{1+R_F}. \tag{56}$$

Because of reflection at the boundaries, some internal reflection of the injected photons will occur. This may be significant if $\tau \approx 1$. This can be accounted for by adjusting the definition of the source term $S(\mathbf{r})$. With infinite multiple reflections between the top and bottom surfaces and normal specular reflection of the injected photons, one finds the source term

$$S(\mathbf{r}) = \frac{\gamma_s{}' S_0\delta(\rho)}{2\pi\rho}\frac{\exp(-\gamma_{tr}z) + R_N\exp\left[-\gamma_{tr}(2t-z)\right]}{1-R_N^2\exp(-2\tau)}, \tag{57}$$

where R_N is the internal normal reflectance of the injected photons, and is evaluated in the Appendix. If $\tau \ge 2$, the expression for $S(\mathbf{r})$ reverts to the previous definition, Eq. 38.

Green's Function Solution

The solution to the diffusion equation, Eq. 44, is found using a Green's function

$$u(\rho, z) = (1/D)\,Ú\,S(\rho', z')\,G(\rho, z; \rho', z')\,\rho'\,d\rho'\,dz', \tag{58}$$

where the Green's function $G(\rho,z; \rho', z')$ is the solution to

$$\begin{aligned}&\left(\nabla^2 - \frac{c\gamma_a}{D}\right)G(\rho,z;\rho',z') = \\ &-\delta(\rho-\rho')\delta(z-z')/(2\pi\rho)\end{aligned} \tag{59}$$

and satisfies the boundary conditions Eqs. 53 and 54. Such a Green's function is given by

$$\begin{aligned}&G(\rho,z;\rho',z') = \\ &\sum_{n=1}^{\infty}\psi_n(z)\psi_n(z')I_0(\sigma_n\rho_</t)K_0(\sigma_n\rho_>/t).\end{aligned} \tag{60}$$

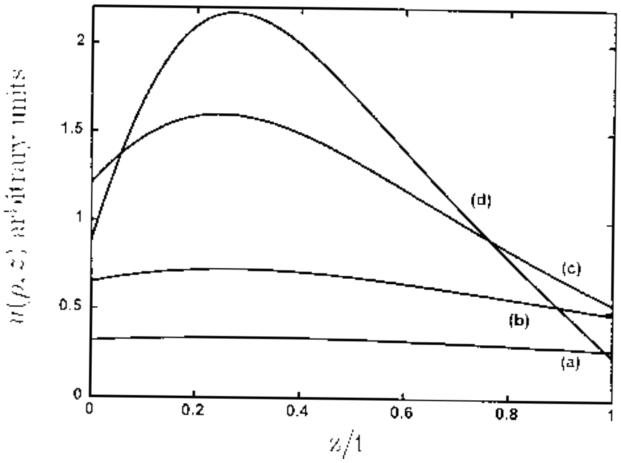

Figure 1. Photon density u(ρ,z) as a function of z in units of t, γ_a = 0, and ρ = 0.5t. The top surface of the paper is z = 0. (a) τ = 1, (b) τ = 2, (c) τ = 4, (d) τ = 8.

The orthonormal eigenfunctions $\psi_n(z)$ defined on the interval [0,*t*] are

$$y_n(z) = A_n \cos(\mu_n z/t - l_n) \tag{61}$$

with normalization factor

$$A_n = \left[\frac{4\mu_n / t}{2\mu_n + \sin 2(\mu_n - \lambda_n) + \sin 2\lambda_n}\right]^{1/2}. \tag{62}$$

The eigenvalues μ_n are determined by

$$\tan \mu_n = \frac{2\tau\delta\mu_n}{\mu_n^2 - (\tau\delta)^2}, \tag{63}$$

and the phase λ_n is given by

$$\cot \lambda_n = \frac{\mu_n}{\tau\delta}. \tag{64}$$

The quantity I_0 and K_0 are modified Bessel functions, σ_n is defined by

$$\sigma_n^2 = \mu_n^2 + 3\gamma_{tr}\gamma_a t^2, \tag{65}$$

and $\rho_<$ is the smaller of ρ, ρ′, and $\rho_>$ the larger.

Using Eqs. 63 and 64, it can be shown that

$$\mu_n = (n-1)p + 2l_n, \tag{66}$$

so that

$$y_n(t) = (-1)^{n+1} y_n(0) \tag{67}$$

and the normalization factor can be written as

$$A_n = \left[\frac{2\mu_n / t}{\mu_n + \sin 2\lambda_n}\right]^{1/2}. \tag{68}$$

Inserting the expression for *S*(**r**), Eq. 57, into Eq. 58, one finds that *u*(ρ,*z*) is

$$\begin{aligned} u(\rho,z) = {} & \frac{S_0}{2\pi D}\frac{1}{1-R_N^2\exp(-2\tau)}\sum_n \frac{\gamma_s{}' t\tau}{\tau^2+\mu_n^2} \\ & \times\Big\{\psi_n(0)\big[(1+\delta) - R_N\exp(-2\tau)(1-\delta)\big] \\ & -\psi_n(t)\exp(-\tau)\big[(1-\delta) - R_N(1+\delta)\big]\Big\}\psi_n(z)K_0(\sigma_n\rho/t), \end{aligned}$$

where we have used the boundary conditions, Eqs. 53 and 54. Figure 1 shows *u*(ρ, *z*) as a function of *z* for several values of optical thickness τ. One sees that the density is maximum some distance inside the paper due to loss of photons at the surface and that the density then decreases at greater depths because of scattering and loss through the lower surface. The lower the optical thickness, the lower the overall density because fewer photons are scattered.

Diffusion Point Spread Function. The diffusion point spread function is equal to the normalized diffuse photon flux from the top surface of the paper. This can be obtained from the partial diffuse photon current in the –*z* direction, given by Eq. 46, at *z* = 0. The diffuse photon flux through the top surface is

$$F_-(\rho) = -(1-R_F)\hat{\mathbf{k}}\cdot\mathbf{j}_-(\rho,0). \tag{70}$$

Using Eq. 47 and the boundary condition Eq. 53, one obtains for the diffuse photon flux

$$F_-(\rho) = \frac{c}{2}\frac{1-R_F}{1+R_F}u(\rho,0). \tag{71}$$

The diffuse reflectance of the paper surface is the total diffuse flux out divided by the flux in, S_0

$$R_p = (1/S_0)\int F_-(\rho)\,dA = \frac{c}{2S_0}\frac{1-R_F}{1+R_F}2\pi\int_0^\infty u(\rho,0)\rho\,d\rho. \tag{72}$$

Using Eq. 69 for *u*(ρ,0), the integral over K_0 evaluates to t^2/σ_n^2. Noting that $(ct/D)(1-R_F)/(1+R_F) = 2\tau\delta$, Eq. 56, that $\cos(\mu_n - \lambda_n) = (-1)^{n+1}\cos\lambda_n$, Eq. 67, and that $\tau\delta\cos\lambda_n/\mu_n = \sin\lambda_n$, Eq. 64, we can define, using Eq. 62

$$\begin{aligned} q_n = {} & \frac{(\gamma'_s t\tau)}{1-R_N^2\exp(-2\tau)}\frac{1}{\tau^2+\mu_n^2}\frac{\mu_n^2\sin 2\lambda_n}{\mu_n+\sin 2\lambda_n} \\ & \times\Big\{\big[(1+\delta) - R_N\exp(-2\tau)(1-\delta)\big] \\ & +(-1)^n\exp(-\tau)\big[(1-\delta) - R_N(1+\delta)\big]\Big\}. \end{aligned} \tag{73}$$

Thus, the reflectance can be expressed as

$$R_p = \sum_n q_n / \sigma_n^2. \tag{74}$$

Note that if τ ≥ 2 and the scattering coefficient is much greater than the absorption coefficient (always true for white paper), then the expression for q_n can be significantly simplified

$$q_n \approx \frac{1+\delta}{1+(\mu_n/\tau)^2}\frac{\mu_n^2\sin 2\lambda_n}{\mu_n+\sin 2\lambda_n}.$$

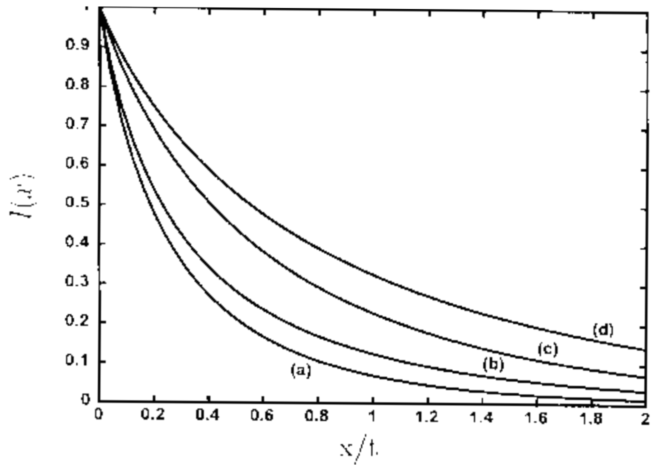

Figure 2. Line spread function l(x), x in units of t. (a) $\gamma_s't = 1.5$ and $\gamma_a t = 0$, (b) $\gamma_s't = 1.5$ and $\gamma_a t = 0.25$, (c) $\gamma_s't = 5.0$ and $\gamma_a t = 0$, (d) $\gamma_s't = 5.0$ and $\gamma_a t = 0.25$. Plots are normalized such that l(0) = 1 for comparison.

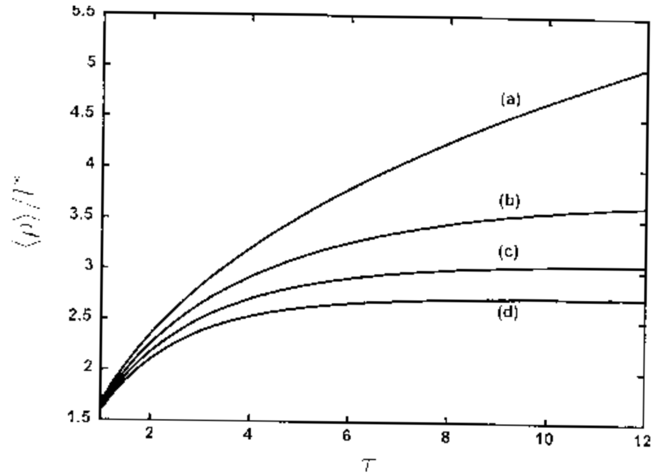

Figure 4. Scattering length <ρ> as a function of optical thickness τ, mean free path constant. <ρ> is in units of mean free path l_*. (a) $\gamma_a = 0$, (b) $\gamma_a = 0.01$, (c) $\gamma_a = 0.02$, (d) $\gamma_a = 0.03$.

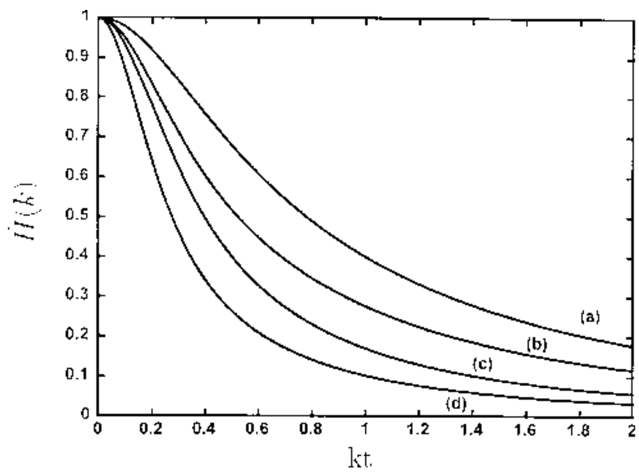

Figure 3. Modulation transfer function $\tilde{H}(k)$, k in units of t^{-1}. (a) $\gamma_s't = 1.5$ and $\gamma_a t = 0$, (b) $\gamma_s't = 1.5$ and $\gamma_a t = 0.25$, (c) $\gamma_s't = 5.0$ and $\gamma_a t = 0$, (d) $\gamma_s't = 5.0$ and $\gamma_a t = 0.25$.

The point spread function is the normalized diffuse photon flux out of the surface

$$H(\rho) = \frac{F\_(\rho)}{2\pi\int_0^\infty F\_(\rho)\rho d\rho}$$

or

$$H(\rho) = \frac{1}{2\pi R_p t^2}\sum_n q_n K_0(\sigma_n \rho / t). \tag{75}$$

That $H(\rho)$ is infinite at the origin is consistent with measurements made of the PSFs of photographic emulsions by Gilmore.[25]

The normalized diffusion line spread function is readily obtained from the point spread function

$$l(x) = \int_{-\infty}^{\infty} H(\rho) dy$$

or, using Eq. 75,

$$l(x) = \frac{1}{2t R_p}\sum_n (q_n / \sigma_n)\exp[-\sigma_n |x| / t]. \tag{76}$$

Figure 2 shows the LSF for various γ_s' and γ_a. For sake of comparison, the functions have been normalized in the figure such that $l(0) = 1$.

The MTF is readily obtained by taking the Fourier transform of $l(x)$ [or the Hankel transform of $H(\rho)$] and is found to be

$$\tilde{H}(k) = \frac{1}{R_p}\sum_i \frac{q_i}{(2\pi kt)^2 + \sigma_i^2}. \tag{77}$$

Figure 3 shows the MTF for the same γ_s' and γ_a as in Fig. 2. Using the definition Eq. 15 one writes $\tilde{H}_{nm}$ as

$$\tilde{H}_{nm} = \frac{1}{R_p}\sum_i \frac{q_i}{(2\pi)^2(n^2+m^2)(t/r)^2 + \sigma_i^2}. \tag{78}$$

The scattering length, defined as the average lateral distance a photon travels before exiting the paper, using Eq. 24 is

$$\langle\rho\rangle = \frac{t\pi}{2R_p}\sum_i q_i / \sigma_i^3. \tag{79}$$

As indicated earlier, $<\rho>^{-1}$ is approximately the spatial bandwidth of the paper. Figure 4 shows a plot of $<\rho>/ l^*$ as a function of the thickness of the paper: $t/l^* = \tau$. In the figure, the mean free path l^* is held constant while the paper thickness t is varied. For a given mean free path, the scattering length increases as the paper thickness increases. If there is no absorption, the scattering length increases without bound as $<\rho> \propto t \to \infty$. The distance the photons migrate is limited by the transmission through the far side as can be inferred from Fig. 1. If absorption occurs, however, the scattering length reaches a limit for $t \to \infty$ as shown in curves 4(b) and 4(c).

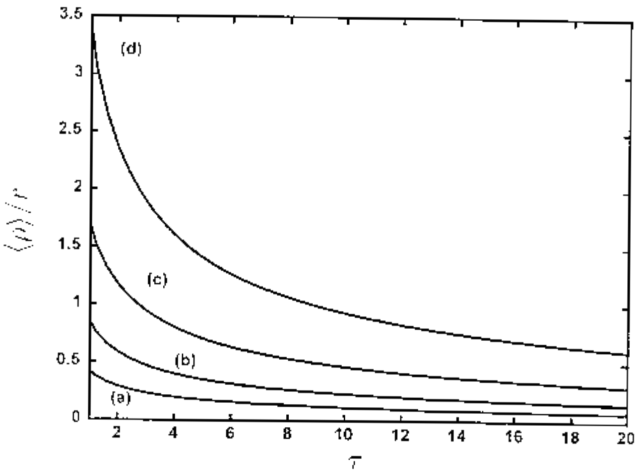

Figure 5. Scattering length <ρ> as a function of optical thickness τ, paper thickness t constant. <ρ> in units of grid period r. (a) t/r = 0.25, (b) t/r = 0.5, (c) t/r = 1.0, (d) t/r = 2.0.

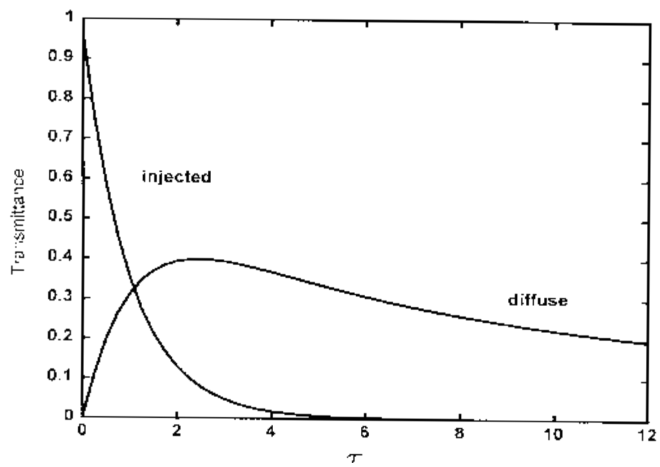

Figure 6. Transmittance of diffuse and injected photons as a function of optical thickness τ with $\gamma_a = 0$.

Figure 5 shows <ρ> as a function of the optical thickness (paper thickness held constant) for several different screen periods, where <ρ> is expressed in units of grid spacing *r*. Recall that the ratio <ρ>/*r* determines the degree of optical dot gain. One sees, as expected, the scattering length decreases with the optical thickness.

Note that our model satisfies the conservation of energy: with $\gamma_a = 0$ the total reflectance plus transmittance is equal to 1. The total reflectance is the diffuse reflectance, Eq. 74, plus the reflectance of the injected photons

$$R_p(\text{injected}) = \frac{(1-R_N)R_N\exp(-2\tau)}{1-R_N^2\exp(-2\tau)},$$

so that the total reflectance is

$$R_p(\text{total}) = \sum_n q_n / \sigma_n^2 + \frac{(1-R_N)R_N\exp(-2\tau)}{1-R_N^2\exp(-2\tau)}. \quad (80)$$

The transmittance is the total flux emitted from the lower surface divided by the incident flux and consists of the diffuse transmittance plus the transmittance of injected photons. The diffuse transmittance is

$$T_p(\text{diffuse}) = (1/S_0)(1-R_F)\int \hat{\mathbf{k}}\cdot\mathbf{j}_-(\rho,t)\,dA. \quad (81)$$

Using Eqs. 47, 54, 69 and 73:

$$T_p(\text{diffuse}) = \sum_n (-1)^{n+1} q_n / \sigma_n^2. \quad (82)$$

The transmittance of injected photons is

$$T_p(\text{injected}) = \frac{(1-R_N)\exp(-\tau)}{1-R_N^2\exp(-2\tau)},$$

so that the total transmittance is

$$T_p(\text{total}) = \sum_n (-1)^{n+1} q_n / \sigma_n^2 + \frac{(1-R_N)\exp(-\tau)}{1-R_N^2\exp(-2\tau)}. \quad (83)$$

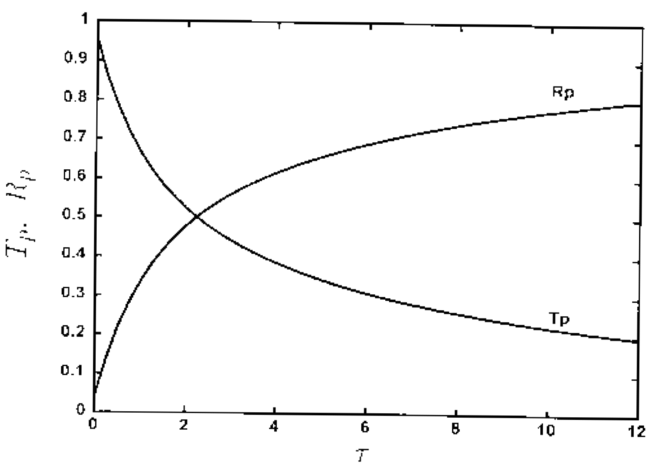

Figure 7. Reflectance and transmittance of diffuse and injected photons as a function of optical thickness τ with $\gamma_a = 0$.

Figure 6 shows the transmittance of injected photons and diffuse photons as a function of τ.

It can be shown numerically using Eqs. 80 and 83 that if $\gamma_a = 0$

$$R_p(\text{total}) + T_p(\text{total}) = 1 \quad (84)$$

independent of any of the paper's other parameters. Figure 7 shows R_p(total) and T_p(total) as a function of τ.

The scattering and absorption coefficients γ_s' and γ_a can be fixed for a particular paper by equating the measured transmittance and reflectance of the paper to the calculated values as given by Eqs. 80 and 83. Using standard techniques,[26] one measures the reflectance of the paper against a black background to get R_p and the reflectance off a stack of papers gives R_∞. The measured transmission is then given by

$$T_p = \sqrt{(1/R_\infty - R_p)(R_\infty - R_p)}. \quad (85)$$

Note that if the specular reflectance is excluded in the measurements of R_p and R_∞, then only the first terms of Eqs. 80 and 83 should be used.

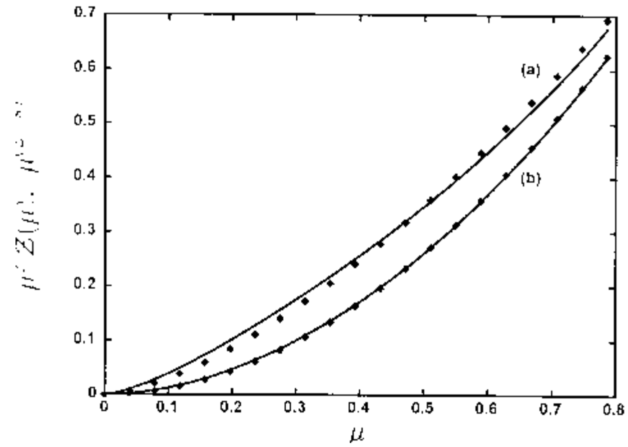

Figure 8. $\mu^2 Z$ and $\mu^{(2-s)}$ as a function of μ; where $\mu^2 Z$ is the line and $\mu^{(2-s)}$ are the boxes. (a) $\gamma_s' = 2$, $\gamma_a = 0$, and $t/r = 1$; (b) $\gamma_s' = 12$, $\gamma_a = 0.2$ and $t/r = 1$.

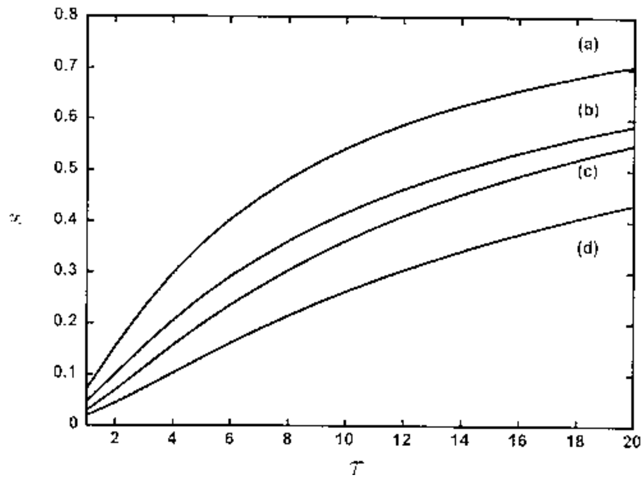

Figure 9. The parameter s as a function of optical thickness τ for various γ_a t/r. (a) $\gamma_a t = 0.2$, $t/r = 0.75$; (b) $\gamma_a t = 0$, $t/r = 0.75$; (c) $\gamma_a t = 0.2$, $t/r = 1.25$; (d) $\gamma_a t = 0$, $t/r = 1.25$.

The calculations of this section have assumed black backing, i.e., none of the transmitted flux is reflected back into the paper. If there is a backing with non-zero reflectance, then the equations of this section must be modified. In fact, flux reflected off the backing decreases the paper's spatial bandwidth. If the paper lies on a surface with reflectance R_b, then some of the outward flux is reflected back into the paper so that the inward flux on the lower surface of the paper is the outward flux multiplied by R_b. The boundary condition for the lower surface is in this case

$$\hat{\mathbf{k}} \cdot \mathbf{j}_-(\rho,t) = R_F \hat{\mathbf{k}} \cdot \mathbf{j}_+(\rho,t) + (1-R_F)R_b \hat{\mathbf{k}} \cdot \mathbf{j}_+(\rho,t), \quad (86)$$

where the first term on the right represents the internally reflected flux and the second term represents the flux reflected by the backing. (This ignores any multiple reflection between the backing and the paper.) Using Eqs. 47 and 43, this can be expressed as

$$\frac{c}{4}u(\rho,t) + \frac{D}{2}\frac{\partial}{\partial z}u(\rho,z)\Big|_{z=t} = \left[R_F + (1-R_F)R_b\right]\left[\frac{c}{4}u(\rho,t) - \frac{D}{2}\frac{\partial}{\partial z}u(\rho,z)\Big|_{z=t}\right]. \quad (87)$$

Defining

$$\delta' = \frac{3}{2}\frac{1 - R_F - R_b + R_F R_b}{1 + R_F + R_b - R_F R_b},$$

one obtains the homogeneous mixed boundary condition for the bottom surface

$$u(\rho,t) + \frac{t}{\tau\delta'}\frac{\partial}{\partial z}u(\rho,z)\Big|_{z=t} = 0. \quad (88)$$

The equation defining the eigenvalues in this case is

$$\tan \mu_n = \frac{\tau(\delta + \delta')\mu_n}{\mu_n^2 - \tau^2\delta\delta'}. \quad (89)$$

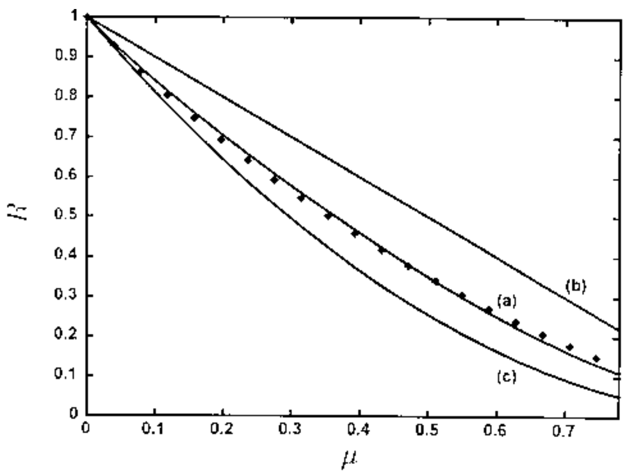

Figure 10. Halftone reflectance as function of percent area covered by ink. (a) Comparison of $\overline{R}$ as calculated with Z (solid line) and μ^{-s} (boxes); $\tau = 12$, $\gamma_a t = 0.2$, and $s = 0.53$. Also shown are the reflectances for no scattering (b) $Z = \mu^{-1}$ ($s = 1$) and complete scattering (c) $Z = 1$, ($s = 0$). The ink transmittance is $T_0 = 0.01$ and $t/r = 1$.

Halftone Reflectance with Diffusion PSF

One is particularly interested in the series Z, Eq. 22, because this factor contains the effects of the optical dot gain. As noted in the discussion preceding Eqs. 25 and 29, if there is no scattering ($\langle\rho\rangle/r \approx 0$) then $Z(\mu) \approx \mu^{-1}$ and for complete scattering ($\langle\rho\rangle/r \gg 1$) $Z(\mu) = 1$. This suggests that Z may be approximated by μ raised to a negative power between 0 and 1:

$$Z(\mu) = \mu^{-s} \quad (90)$$

with

$$0 \le s \le 1. \quad (91)$$

In fact, this is a very good approximation for Z as calculated with the diffusion PSF. Figure 8 shows the curves $\mu^2 Z(\mu)$ and μ^{2-s} versus μ for a moderate degree of optical dot gain. The parameter $1 - s$ is an index of optical dot gain. If $1 - s = 0$, no scattering and no optical dot gain occur (see Eq. 30), and for $1 - s = 1$ the light is "completely" scattered and maximum optical gain occurs (see Eq. 26). Figure 9 shows the parameter s as a function of τ for several t/r.

Figure 10 shows the halftone reflectance Eq. 21 using the diffusion PSF. Also shown in the figure are Eqs. 30 and 27 for the case of no scattering and complete scattering for comparison. Also shown is the reflectance with a best fit s in μ^{2-s}. In all curves, the halftone reflectance in given in terms of the paper reflectance $\overline{R} / R_p$.

Dot and Non-Dot Reflectance

There has been some interest in expressing optical dot gain in terms of an expanded Murray-Davies model.[4] In this model, the average reflectance of inked areas $\overline{R}_i(\mu)$ and noninked areas $\overline{R}_n(\mu)$ are functions of dot size. In the following, we express the expanded Murray-Davies model in terms of the theory developed here and use this model to give a physical interpretation of the series Z.

The total reflectance from a region is the sum of $\overline{R}_i(\mu)$ and $\overline{R}_n(\mu)$, weighted by their relative contributions

$$\overline{R} = \mu \overline{R}_i(\mu) + (1-\mu)\overline{R}_n(\mu), \tag{92}$$

where μ is the fractional area covered by ink and $1 - \mu$ is the noninked area. One can find $\overline{R}_i(\mu)$ and $\overline{R}_n(\mu)$ by averaging $R(x,y)$ over the inked and noninked areas, respectively

$$\overline{R}_i(\mu) = \frac{1}{\mu (Nr)^2} \int C(x,y) R(x,y) dA \tag{93}$$

and

$$\overline{R}_n(\mu) = \frac{1}{(1-\mu)(Nr)^2} \int (1 - C(x,y)) R(x,y) dA, \tag{94}$$

where $\mu(Nr)^2$ is the area that is inked; $C(x,y)$ is 1 if the point x,y is in an inked area and 0 otherwise, Eq. 4; and $R(x,y)$ is the point reflectance, Eq. 7. Note that

$$[C(x,y)]^2 = C(x,y)$$

and

$$\frac{1}{(Nr)^2} \int C(x,y) dA = \mu,$$

$$\frac{1}{(Nr)^2} \int C(x,y) P(x,y) dA = \mu^2 Z(\mu)$$

Carrying out the integration in Eqs. 93 and 94, one obtains

$$\overline{R}_i(\mu) = R_p T_0 [1 - (1 - T_0)\mu Z] \tag{95}$$

and

$$\overline{R}_n(\mu) = R_p \left[1 - (1 - T_0) \frac{\mu}{1-\mu} (1 - \mu Z) \right]. \tag{96}$$

By examining these expressions for $\overline{R}_i(\mu)$ and $\overline{R}_n(\mu)$, one can infer a physical meaning for the series Z.

The physical interpretation of Z is motivated by considering the probabilities that a photon is reflected from an inked or a noninked region. We can define $P_R(i)$ [or $P_R(n)$] as the probability that a photon is reflected from an inked [or noninked] area and $P_I(i)$ [or $P_I(n)$] as the probability that a photon is incident on an inked [or noninked] area. We can define the conditional probability $P(i|i)$ [or $P(i|n)$] as the probability that if a photon originally entered the paper through an inked area, it exits the paper through an inked [or noninked] area and $P(n|i)$ [or $P(n|n)$] as the probability that if the photon originally entered the paper through a noninked area, it exits the paper through an inked [or noninked] area. To value T_0 can be interpreted as the conditional probability that if a photon enters or exits an inked area, it is transmitted through the ink. Then the following relations hold

$$P_R(i) = P_I(n)\, P(n|i)\, T_0 + P_I(i)\, P(i|i)\, T_0^2, \tag{97}$$

$$P_R(n) = P_I(n)\, P(n|n) + P_I(i)\, P(i|n)\, T_0. \tag{98}$$

(For simplicity, we let $R_p = 1$.) Clearly,

$$P_I(i) = \mu, \qquad P_I(n) = 1 - \mu \tag{99}$$

and

$$P_R(i) = \mu \overline{R}_i(\mu) \qquad P_R(n) = (1-\mu)\overline{R}_n(\mu). \tag{100}$$

The conditional probabilities are related in that

$$P(i|i) + P(i|n) = 1, \tag{101}$$

$$P(n|i) + P(n|n) = 1, \tag{102}$$

and a "detailed balance" holds

$$P_I(i)\, P(i|n) = P_I(n)\, P(n|i). \tag{103}$$

If we define $\beta = P(i|i)$, then by Eq. 101

$$P(i|n) = 1 - \beta \tag{104}$$

and by Eqs. 99 and 103

$$P(n|i) = \frac{\mu}{1-\mu}(1-\beta) \tag{105}$$

and by Eq. 102

$$P(n|n) = 1 - \frac{\mu}{1-\mu}(1-\beta). \tag{106}$$

Inserting Eqs. 104 through 106 into Eqs. 97 and 98 one obtains

$$\overline{R}_i(\mu) = T_0[1 - (1 - T_0)\beta], \tag{107}$$

$$\overline{R}_n(\mu) = 1 - (1 - T_0)\frac{\mu}{1-\mu}(1-\beta). \tag{108}$$

Comparison of Eqs. 107 and 108 with Eqs. 95 and 96 shows that $\beta = \mu Z$; one interprets μZ as the probability that a photon on entering a dot will exit through the dot. Specifically, we can interpret Z^{-1} as an effective scattering area $Z^{-1} = \mu_{scat}$. The scatter of photons within the paper increases the size of the area from which the photon might exit the paper after having entered through a dot. This larger area is the scattering area μ_{scat}. The probability that a photon exits through the dot is the ratio of the dot size μ to the scattering size μ_{scat}, $P(i|i) = \mu/\mu_{scat}$. Hence, if $Z^{-1} = \mu$, the scattering area is the same as the physical dot size: no optical dot gain. If $Z^{-1} = 1$, then the scattering area is equal to the size of the screen cell: the photons are completely scattered.

As indicated above, Eq. 90, μ^s is a good approximation to $1/Z$ when Z is calculated using the diffusion PSF. When this approximation is used the dot and nondot reflectances are

$$\overline{R}_i(\mu) = R_p T_0 [1-(1-T_0)\mu^{1-s}] \tag{109}$$

and

$$\overline{R}_n(\mu) = R_p [1-(1-T_0)\frac{\mu}{1-\mu}(1-\mu^{1-s})]. \tag{110}$$

The expression for $\overline{R}_i(\mu)$ is identical to the phenomenological expression used by Arney et al.[4] to fit their data. The expression for $\overline{R}_n(\mu)$ is not the same as theirs, however, the difference in numerical value is small.

Conclusion

In the preceding, we have developed a theory of optical dot gain. The theory is expressed in terms of an effective dot size Z^{-1}, which is a measure of the migration of photons within paper. We have derived a PSF by solving the transport equation in the diffusion approximation. The PSF is a function of two experimentally determined parameters that describe the scattering and absorption characteristics of the paper.

Several ways exist to improve the model. We assumed that the paper was homogeneous and isotropic, which is clearly not the case for real papers. In real papers a significant degree of flocculation exists that results in local variation in grammage. In addition, the paper-forming process gives significant orientation to the fibers that results in directionality. There has been a lot of recent work on the statistics of fiber distribution,[23,24] and an improvement in our model would incorporate this work.

As indicated earlier, the paper fibers are flattened with a width-to-thickness ratio of 10 and the fibers lie in the plane of the paper. This results in a layered structure with transport properties in the vertical direction different from those in the horizontal direction. This structure is dealt with only partially in the current theory. In particular, the internal reflection within the fibers will be significantly different in the two directions. This difference in internal reflection tends to increase the horizontal flow of scattered photons over the vertical; the net flow of photons in the plane of the paper is greater than that in the perpendicular direction. For a given transmission, this will result in a decreased spatial bandwidth. An improved model would take into consideration this layered structure of paper.[27]

In addition, we are currently applying the theory to a color halftone print.

Appendix

In the following we show how internal reflectance within paper can be characterized by an effective reflectance coefficient,[19] and expressed in terms of a boundary condition.

For papers considered here, the volume ratio of air to fiber is approximately 1. We can, therefore, take the paper medium as cellulose and consider the internal reflectance that occurs at the paper surfaces when light passes from within the paper to outside the paper. Including internal reflection partially accounts for the layered structure of paper. The reflectance is given by the Fresnel reflection coefficient, which is a function of the angle at which the photons approach the surface. This reflected flux can be considered incoming at the surface, so that the partial current into the paper at the surface is equal to the outgoing flux times the Fresnel reflectance. Our treatment closely follows that of Haskell et al.,[19] except here we include the effects of a rough surface.

Effective reflectance can be obtained by averaging over all angles. For the top surface this is, using Eq. 46,

$$\begin{aligned}&\hat{\mathbf{k}}\cdot\mathbf{j}_+(\rho,0) = \\ &c\int_{\hat{\mathbf{s}}\cdot\hat{\mathbf{n}}\geq 0} R_F(\theta) f_d(\rho,0;\hat{\mathbf{s}})\hat{\mathbf{s}}\cdot\hat{\mathbf{n}}\,d\Omega,\end{aligned} \tag{A1}$$

where θ is defined by $\cos\theta = \hat{\mathbf{s}}\cdot\hat{\mathbf{n}}$, with $\hat{\mathbf{n}}$ the (outward) unit vector normal to the surface. The value $R_F(\theta)$ is the Fresnel reflection coefficient for unpolarized light

$$\begin{aligned}R_F(\theta) &= \frac{1}{2}\left(\frac{\sin(\theta-\theta')}{\sin(\theta+\theta')}\right)^2 + \frac{1}{2}\left(\frac{\tan(\theta-\theta')}{\tan(\theta+\theta')}\right)^2, \\ &\text{if} \quad 0 \leq \theta \leq \theta_c \\ &= 1, \quad \text{if} \quad \theta_c \leq \theta \leq \pi/2\end{aligned} \tag{A2}$$

where θ' is given by Snell's Law $n \sin\theta = \sin\theta'$, n is the index of refraction of cellulose $n = 1.5$, and θ_c is the critical angle for total internal reflection given by $\sin\theta_c = 1/n$.

Eq. A1 is a good approximation only if the normal is parallel to the z axis. In fact, the (uncoated) paper surface is rough and the surface normal $\hat{\mathbf{n}}$ will vary from point to point. This tends to decrease the effective Fresnel reflectance. An effective reflectance is more accurately obtained by averaging Eq. A1 over $\hat{\mathbf{n}}$. One can define a normalized probability density $P(\hat{\mathbf{n}})$ that gives the probability per unit solid angle that the normal has direction $\hat{\mathbf{n}}$. By our assumption of paper isotropy, $P(\hat{\mathbf{n}})$ is independent of the azimuthal angle f and can be written

$$P(\hat{\mathbf{n}}) = \frac{1}{2\pi}P(\cos\theta_{\hat{\mathbf{n}}}),$$

where $\theta_{\hat{\mathbf{n}}}$ is defined by $\cos\theta_{\hat{\mathbf{n}}} = \hat{\mathbf{n}}\cdot\hat{\mathbf{k}}$

Averaging Eq. A1 over $\hat{\mathbf{n}}$,

$$\hat{\mathbf{k}} \cdot \mathbf{j}_{+}(\rho,0) = c\int_{\hat{\mathbf{n}}\cdot\hat{\mathbf{k}}\geq 0} \int_{\hat{\mathbf{s}}\cdot\hat{\mathbf{n}}\geq 0} R_F(\theta_{\hat{\mathbf{s}}}) f_d(\rho,0;\hat{\mathbf{s}})\hat{\mathbf{s}}\cdot\hat{\mathbf{n}}P(\hat{\mathbf{n}})d\Omega_{\hat{\mathbf{s}}}d\Omega_{\hat{\mathbf{n}}}, \tag{A3}$$

and expanding both sides of Eq. A3 using Eqs. 39 and Eq. 47, one obtains

$$\frac{c}{4}u(\rho,0) + \frac{1}{2}\hat{\mathbf{k}}\cdot\mathbf{j}(\rho,0) = R_u\frac{c}{4}u(\rho,0) - \bar{n}_z R_j \frac{1}{2}\hat{\mathbf{k}}\cdot\mathbf{j}(\rho,0), \tag{A4}$$

where

$$R_u = 2\int_0^{\pi/2} R_F(\theta)\cos\theta\sin\theta\, d\theta,$$

$$R_j = 3\int_0^{\pi/2} R_F(\theta)\cos^2\theta\sin\theta\, d\theta,$$

and

$$\bar{n}_z = \int_0^{\pi/2} \cos\theta\sin\theta P(\cos\theta)\,d\theta,$$

which can be written as

$$\frac{c}{4}u(\rho,t) + \frac{1}{2}\frac{1+\bar{n}_z R_j}{1-R_u}\hat{\mathbf{k}}\cdot\mathbf{j}(\rho,t) = 0. \tag{A5}$$

Defining the effective Fresnel reflection coefficient as

$$R_F = \frac{\bar{n}_z R_j + R_u}{2 + \bar{n}_z R_j - R_u}, \tag{A6}$$

this becomes

$$\frac{c}{4}u(\rho,0) + \frac{1}{2}\frac{1+R_F}{1-R_F}\hat{\mathbf{k}}\cdot\mathbf{j}(\rho,0) = 0 \tag{A7}$$

or

$$\hat{\mathbf{k}}\cdot\mathbf{j}_{+}(\rho,0) = -R_F\hat{\mathbf{k}}\cdot\mathbf{j}_{-}(\rho,0). \tag{A8}$$

One analyzes the bottom surface in a similar manner to obtain, using Eq. 45

$$\hat{\mathbf{k}}\cdot\mathbf{j}_{+}(\rho,t) = R_F\hat{\mathbf{k}}\cdot\mathbf{j}_{-}(\rho,t). \tag{A9}$$

To evaluate R_F, one must choose a suitable $P(\cos\theta)$. If the paper is coated, then $P(\cos\theta)\sin\theta d\theta = P(x)\, dx = \delta(x - 1)dx$, with $P(x)$ defined on the interval [0,1]. In this case (flat surface) obviously $\bar{n}_z = 1$. Even for uncoated paper one expects that $P(x)$ is sharply peaked at $x = 1$, because the fibers are flattened in the paper-making process.[24]

A simple model of the noncoated paper surface treats the fibers as elliptical rods, i.e., rods with elliptical cross section lying in the plane perpendicular to the z axis and the major axis also in the plane perpendicular to the z axis.[22] The average z component of the normal is then found by averaging over the upper half of the elliptical curve. Assuming uniform probability for the angle that parameterizes the elliptic curve, a straightforward calculation gives

$$\bar{n}_z = \frac{2}{\pi}\frac{\varepsilon}{\sqrt{\varepsilon^2 - 1}}\arctan\sqrt{\varepsilon^2 - 1},$$

with ε the ratio of the major to minor radii. One sees that the flatter the fiber is ($\varepsilon \to \infty$), then $\bar{n}_z \to 1$. The ratio of fiber width to thickness is typically[24] $\varepsilon = 10$, and one obtains $\bar{n}_z = 0.941$.

With this value of $\bar{n}_z$, and the index of refraction for cellulose $n = 1.5$, one obtains for R_F the value $R_F = 0.574$.

We need also the reflectance for the injected photons R_n. By our model, these photons are normally incident on the paper surface and the reflectance is given by Eq. A2 for $\theta = 0$, or

$$R_N = \left(\frac{n-1}{n+1}\right)^2 = 0.04. \tag{A10}$$

Nomenclature

A_n	=	normalization factor for $y_n(z)$, Eq. 62
circ $[u/d]$	=	shape function for circular dots, Eq. 6
$C(x,y)$	=	array function equal to 1 if point x,y is covered by ink and 0 otherwise. It is a convolution of the dot distribution function and the dot shape function, Eq. 4
d	=	radius of circular dots
D	=	diffusion coefficient, Eq. 44
δ	=	a parameter that expresses the effective increase in mean free path due to internal reflection, Eq. 56
$f(\mathbf{r}, \mathbf{s})$	=	photon distribution, Eq. 35
$f_i(\mathbf{r}, \mathbf{s})$	=	injected photon distribution, Eq. 36
$f_d(\mathbf{r}, \mathbf{s})$	=	diffuse photon distribution, Eq. 39
$F_{-}(\rho)$	=	diffuse photon flux through paper top surface, Eq. 70
g	=	anisotropy parameter for phenomenological phase function, Eq. 32
$g(x,y)$	=	dot distribution function, Eq. 5
$G(\rho,z;\rho',z)$	=	Green's function solution to diffusion equation, Eq. 60
γ_s, γ_a	=	scattering and absorption coefficients for paper, Eq. 31
γ_s'	=	effective scattering coefficient, does not include forward scattered photons, Eq. 34
γ_{tr}	=	transport coefficient, inverse of transport mean free path, Eq. 34
$H(\rho)$	=	radial point spread function (PSF), Eqs. 2 and 75
$\tilde{H}(k)$	=	modulation transfer function (MTF), Fourier transform of the PSF, Eqs. 12 and 77
$\tilde{H}_{nm}$	=	MTF evaluated at $k = \sqrt{n^2 + m^2}/r$, Eqs. 15 and 78
$\mathbf{j}(\mathbf{r})$	=	diffuse photon current density, Eq. 41
$\mathbf{j}_{\pm}(\mathbf{r})$	=	partial photon current densities, Eqs. 45 and 46
J_{nm}	=	Fourier transform of dot shape function normalized to $J_{00} = 1$, evaluated at $k = \sqrt{n^2 + m^2}/r$, Eqs. 14 and 23
k	=	spatial frequency in lines/unit length
K_0	=	modified Bessel function of the second kind
l^*	=	transport mean free path, distance over which velocity relaxes
$l(x)$	=	line spread function, Eq. 76
λ_n	=	phase of $y_n(z)$, Eq. 64

μ = dot area fraction

μ_n = eigenvalue of longitudinal differential operator, Eq. 63

n = Yule-Nielson n-parameter (section on Halftone Reflectance only); index of refraction (everywhere else)

$P_R(a), P_I(a)$, = probability a photon is reflected from or incident on region a, with $a = i$ (inked) or n (noninked), Eqs. 99 and 100

$P(a|b)$ = probability that if photon enters paper through a it exits paper through b, Eqs. 97 and 98

$p(\mathbf{s}, \mathbf{s}¢)$ = phase function, which is the normalized differential scattering cross section, Eq. 32

$\psi_n(z)$ = orthonormal eigenfunction in Green's function expansion, Eq. 61

q_n = expansion coefficient for diffusion PSF, Eq. 73

r = screen period

$R(x,y)$ = reflectance at x,y, Eq. 22

$\overline{R}$ = reflectance averaged over a region, Eq. 21

$\overline{R}_i$ = average reflectance of inked regions, Eq. 93

$\overline{R}_n$ = average reflectance of non-inked regions, Eq. 94

R_p = reflectance of bare paper, Eq. 74

R_F = effective Fresnel reflection coefficient, Eq. A6

R_N = internal normal reflectance of injected photons, Eq. A10

$<\rho>$= lateral scattering length, Eqs. 24 and 79

$S(\mathbf{r})$= source function for diffuse photons, Eq. 38

s_n = eigenvalue of radial differential operator, Eq. 65

t = paper thickness

$T(x,y)$ = transmittance of ink layer at x,y, Eq. 23

T_0 = transmittance of ink

T_p = paper transmittance, Eq. 83

t = optical thickness of paper, number of transport mean free paths in paper thickness, Eq. 55

$u(\mathbf{r})$= diffuse photon density, Eq. 69

Z = Z-series, Eq. 22

References

1. J. S. Arney, C. D. Arney, P. G. Engeldrum, *J. Imaging Sci. Technol*. **40**, 233 (1996); ***see pg. 432, this publication***.
2. P. G. Engeldrum, *J. Imaging Sci. Technol*. **40**, 239 (1996); ***see pg. 426, this publication***.
3. J. S. Arney, C. D. Arney and Miako Katsube, *J. Imaging Sci. Technol*. **40**, 19 (1996).
4. J. S. Arney, P. G. Engeldrum and H. Zeng, *J. Imaging Sci. Technol*. **39**, 502 (1995); ***see pg. 390, this publication***.
5. P. G. Engeldrum and B. Pridham, *TAGA Proc*. 339, 1995.
6. J. A. C. Yule and W. J. Nielsen, *TAGA Proc*. **3**, 65, 1957.
7. K. Case and P. Zweifel, *Linear Transport Theory*, Addison Wesley, Reading, Mass., 1967.
8. A. Ishimaru, *Wave Propagation and Scattering in Random Media*, Academic Press, New York, 1978.
9. F. R. Ruckdeschel and O. G. Hauser, *Appl. Opt*. **17**, 3376 (1978).
10. J. W. Goodman, *Introduction to Fourier Optics*, McGraw-Hill, New York, 1968.
11. J. C. Dainty and R. Shaw, *Image Science*, Academic Press, New York, 1974.
12. A. Murray, *J. Franklin Inst.* **221**, 721 (1936).
13. R. A. J. Groenhuis, H. A. Ferwerda and J. J. Ten Bosch, *Appl. Opt.* **22**, 2456 (1983).
14. A. Ishimaru, *Appl. Opt*. **28**, 2210 (1989).
15. A. Ishimaru, Y. Kuga, R. L.-T. Cheung, and K. Shimizu, *J. Opt. Soc. Amer*. **73**, 131 (1983).
16. K. Furutsu, *J. Opt. Soc. Amer*. **70**, 360 (1980).
17. L. Reynolds, C. Johnson and A. Ishimaru, *Appl. Opt*. **15**, 2059 (1976).
18. J. X. Zhu, D. J. Pine and D. A. Weitz, *Pys. Rev. A* **44**, 3948 (1991).
19. R. Haskell, L. O. Svaasand, T. T. Tsay, T. C. Feng, M. S. McAdams, and B. J. Tromberg, *J. Opt. Soc. Amer. A* **11**, 2727 (1994).
20. R. A. Bolt and J. J. Ten Bosch, in *Waves in Random Media*, **4**, 233 (1994).
21. B. Scott, J. Abbott and S. Trosset, in *Properties of Paper,* TAPPI Press, Atlanta, Georgia, 1995.
22. Paper: *An Engineered Stochastic Structure*, M. Deng and C. T. J. Dodson, Eds., TAPPI Press, Atlanta, 1994.
23. *Handbook of Paper Science*, H. F. Rance, Ed., Elsevier, New York, 1982.
24. *Paper: Structure and Properties*, J. A. Bristow and P. Kolseth, Eds., Marcel Dekker, Inc., New York, 1986.
25. H. F Gilmore, *J. Opt. Soc. Amer.* **57**, 75 (1967).
26. G. Kortüm, *Reflectance Spectroscopy,* Springer-Verlag, New York, 1969.
27. M. Keijzer, W. M. Star and P. R. M. Storchi, *Appl. Opt*. **27**, 1820 (1988).

❋ Previously published in the *Journal of Imaging Science and Technology* **41**(6), pp. 643–656, 1997.